CRYSTAL GROWTH & DESIGN
2004
VOL. 4, NO. 6
1175−1180

In Situ Monitoring of the Impact of Liquid−Liquid Phase Separation on Drug Crystallization by Seeding

Laurent Lafferrère,[†,#] Christian Hoff,[‡] and Stéphane Veesler*[,†]

Centre de Recherche en Matière Condensée et Nanosciences, CRMCN-CNRS, Campus de Luminy, Case 913, F-13288 Marseille Cedex 09, France, and Sanofi-Synthélabo Chimie, F-30390 Aramon, France

Received July 8, 2004; Revised Manuscript Received August 31, 2004

ABSTRACT: In a previous paper (Veesler, S.; Lafferrere, L.; Garcia, E.; Hoff, C. *Org. Proc. Res. Dev.* **2003**, *7*, 983), the impact of a liquid−liquid-phase separation (LLPS) or demixing on solution crystallization in quiescent medium of a pharmaceutical compound, $C_{35}H_{41}Cl_2N_3O_2$, in an ethanol/water mixture was presented. In this contribution, drug crystallization experiments by seeding are monitored by in situ turbidity, focused beam reflectance measurement, and video microscopy. Two cases are studied: in the first case for seeding experiments in the metastable zone for nucleation and outside the demixion zone we observe the classical secondary nucleation and growth mechanism. In the second case for seeding experiments in the demixion zone, the first stage is the growth of crystals as well as the growth and coalescence of droplets; in the second stage crystals and droplets are still growing and droplet heterogeneous nucleation occurs; and in the last stage, droplets disappear and the secondary nucleation starts. LLPS changes the medium and the conditions of crystallization, prevents the drug nucleation, both primary and secondary, and consequently affects the process. Depending on the point of seeding in the phase diagram, inside or outside the LLPS region, the crystallization mechanisms and kinetics are different.

1. Introduction

In the design and study of the crystallization process, knowledge of the factors governing particle size distribution, crystal habit, and phases, namely, polymorphs or solvates, is an important consideration. In many cases, the end products strongly depend on the starting position in the phase diagram, which requires a deep understanding of the phase diagram.[1] Three types of phase diagrams occur naturally depending on the range of the molecular substance interaction.[1−4] For simple hard spheres, only fluid and crystal phases are present (type 1), while introducing attractive interactions results in three-phase equilibria gas−liquid-crystal (type 2), and with shorter-range attractions the gas−liquid or fluid−fluid equilibrium becomes metastable (type 3). Thus, the phase diagram must be determined.[5] For instance, a type 2 phase diagram is observed and described for emulsification and crystallization of lauric acid in an ethanol/water mixture.[6] Type 3 phase diagram is often observed in protein systems;[7,8] however, only two cases are documented for small molecules.[9−11] In this paper, we present a study of the impact of a liquid−liquid-phase separation (LLPS) or demixing on solution crystallization by seeding of a pharmaceutical compound, $C_{35}H_{41}Cl_2N_3O_2$, in an ethanol/water mixture. This compound has previously been studied for its polymorphism and LLPS,[5,9,11] and LLPS is metastable with respect to the crystal−liquid-phase separation (type 3). Furthermore, the occurrence of an LLPS in the nucleation metastable zone was shown to be due to the use of a solvent mixture.[5] LLPS competes with crystal formation affecting the crystallization process.[5,12,13] Thus, the nucleation ability of the substance is sometimes poor; this can be avoided by seeding.[14]

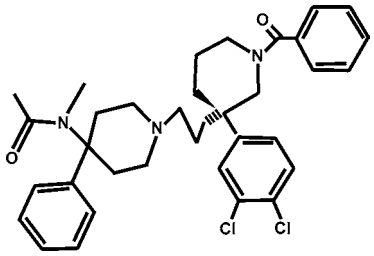

Figure 1. Structure of $C_{35}H_{41}Cl_2N_3O_2$, M. W.: 606.6 g mol^{-1}.

In this study, seeding experiments are carried out in a 200-mL stirred batch-crystallizer in which the turbidity of the suspension and particle size are measured in situ by optical turbidometric and focused beam reflectance (FBRM), respectively. In addition, complementary experiments are performed in a 2-mL quiescent thermostated crystallizer placed under a video microscope, to visualize crystal and droplet evolution. LLPS changes the medium and the conditions of crystallization, prevents drug nucleation, both primary and secondary, and consequently affects the process.

2. Materials and Methods

2.1. Materials. The pharmaceutical compound studied is an organic molecule with the basic formula $C_{35}H_{41}Cl_2N_3O_2$ (Figure 1). This compound crystallizes into two polymorphs, FI and FII, with platelet crystal and needle habit, respectively.[9] FI is monoclinic, whereas FII is orthorhombic. The crystallization process requires an ethanol/water mixture (54.2/45.8% weight) as solvent. Note that the solubility of the polymorphs is high in ethanol but very low in water.

2.2. Solid Characterization. Crystals were observed under a scanning electron microscope (SEM) JEOL 6320F. Moreover, all the solid phases were characterized by X-ray diffraction INEL CPS 120.

* Corresponding author. Phone: 336 6292 2866. Fax: 334 9141 8916. E-mail: veesler@crmcn.univ-mrs.fr.
† CRMCN-CNRS (Laboratory associated with the Universities Aix-Marseille II and III).
‡ Sanofi-Synthélabo Chimie.
# Present address: Oril Industrie 13 rue Auguste Desgenetais BP17 F-76210 BOLBEC, France.

10.1021/cg0497750 CCC: $27.50
Published on Web 10/07/2004

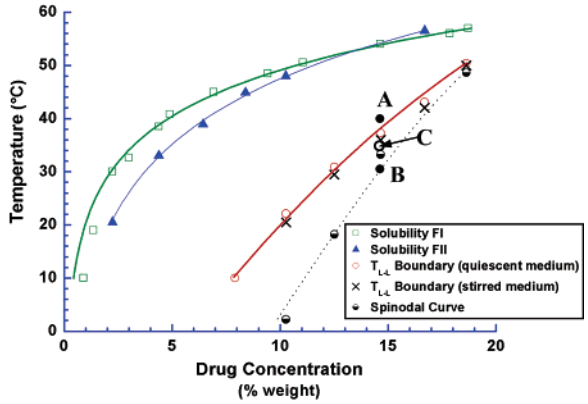

Figure 2. T_{L-L} boundary (quiescent and stirred medium), spinodal curve, and solubility of polymorphs F_I and F_{II} in mixture ethanol/water (54.2/45.8% weight).

2.3. Experimental Setup. Experiments were carried out using a 200-mL batch-crystallizer which was a double-jacketed glass vessel equipped with four wall baffles to prevent the solution from rotating in the crystallizer. We used a three-blade stainless steel propeller (Mixell TT) to stir at a constant speed of 500 rpm. The crystallizer can be rapidly set to different temperatures using a computer-controlled thermostated circulating water bath (Julabo F25). The temperature and turbidity of the solution or the slurry were measured in situ by a platinum resistance thermometer (PT100) and a Mettler-Toledo FSC 402 equipped with a OFS12H-407N Mettler-Toledo probe, respectively. We developed a program using LabVIEW software (National Instruments) to acquire and monitor data. The in situ FBRM technique was used to measure particle size in the range 0.8−1000 μm. For papers dealing with this technique, see Monnier[15] (method and experimental problems), Braatz[16,17] (crystallization applications), and Dowding[18] (emulsion applications). In this work, the focal point of the Lasentec probe was positioned 0.02 mm inside the sapphire window using a FBRM 6B12 Lasentec DL600 instrument. FBRM can be used to give relative measurements without prior calibration as in this study. The advantage of this method is that it analyzes particle size in situ and in real time, without the need for sampling or dilution. In addition, complementary experiments were performed in a 2-mL quiescent thermostated crystallizer placed under a video microscope, to interpret the FBRM data.

A particle vision and measurement 700 (PVM) probe from Mettler-Toledo, an in-process video microscope system for use in crystallization slurries, was also tested in this work for the characterization of the LLPS.

3. Results

3.1 Characterization of the LLPS of $C_{35}H_{41}Cl_2N_3O_2$. The previous study on the LLPS or demixing of $C_{35}H_{41}Cl_2N_3O_2$ in an ethanol/water mixture was performed in a quiescent medium.[5,9,11] Here, we present the temperature-induced LLPS characterization in a 200-mL stirred medium to test different in-process systems as well as the impact of the stirring and the cooling rate on the LLPS. This compound exhibits an LLPS in the metastable zone for crystallization (Figure 2). This separation of a solute-and-ethanol-rich liquid-phase precedes and prevents crystal nucleation of both polymorphs FI and FII. The complete phase diagram was presented in a previous paper.[11]

3.1.1. Comparison of Turbidity and FBRM Probes. The two techniques, turbidity and FBRM probes, used to measure the cloud and clarify points have the same physical principle, i.e., measure of the backscattered light. As expected, both techniques give the same results (Figures 3 and 4). Consequently, in the following the liquid−liquid coexistence curve, in a stirred medium, is measured with the turbidity probe; data are compared with those obtained previously by

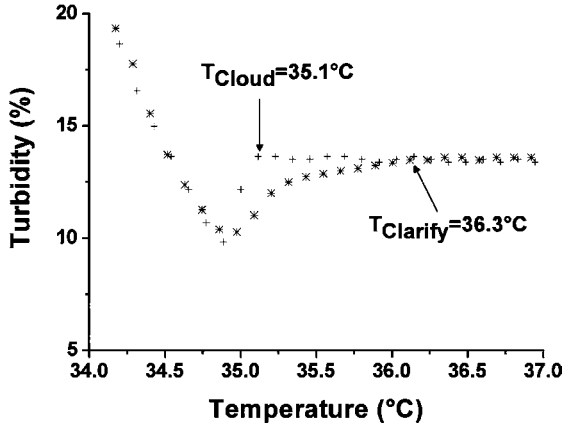

Figure 3. LLPS characterized by turbidity in a stirred drug solution concentrated to 14.6% weight in mixture ethanol/water (54.2/45.8% weight) at cooling (clouding) and heating (clarifying) rates of 1 °C h^{-1}.

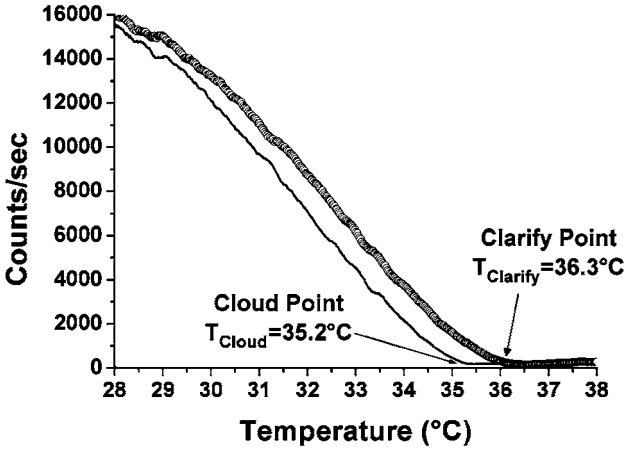

Figure 4. LLPS characterized by FBRM in a stirred drug solution concentrated to 14.6% weight in mixture ethanol/water (54.2/45.8% weight) at cooling (clouding) and heating (clarifying) rates of 1 °C h^{-1} (chord length 1−20 μm).

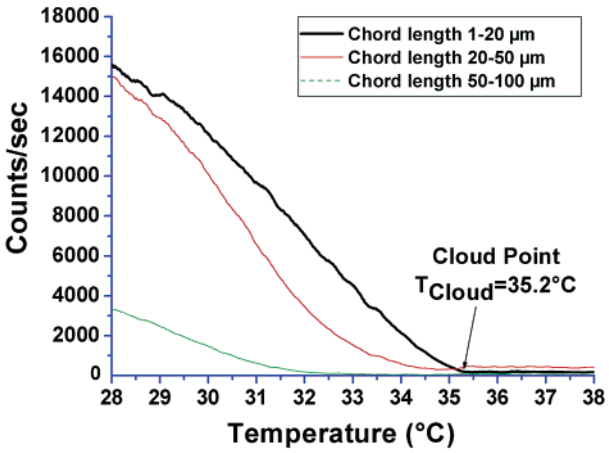

Figure 5. LLPS characterized by FBRM in a stirred drug solution concentrated to 14.6% weight in mixture ethanol/water (54.2/45.8% weight) at a cooling rate of 1 °C h^{-1}.

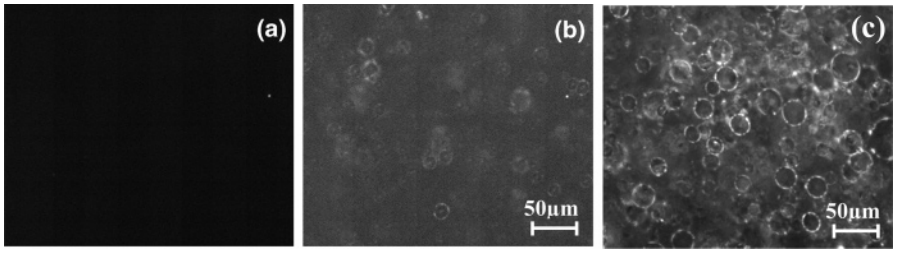

Figure 6. LLPS characterized by PVM in a stirred drug solution concentrated to 14.6% weight in mixture ethanol/water (54.2/45.8% weight) at a cooling rate of 1 °C h^{-1} (a) clear solution at 40 °C, (b) droplet nucleation at 36 °C, and (c) larger droplets at 35 °C.

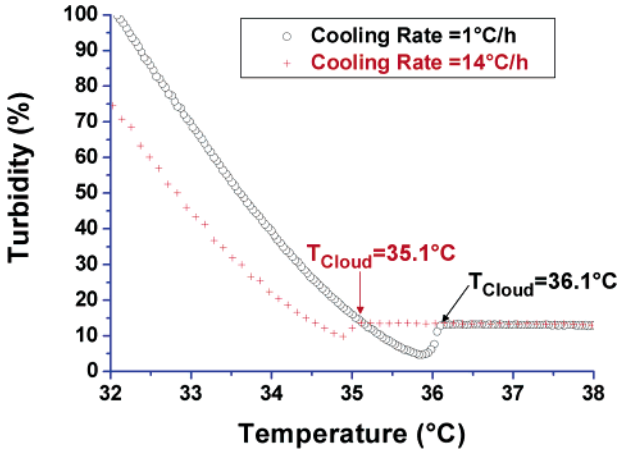

Figure 7. LLPS characterized by turbidity in a stirred drug solution concentrated to 14.6% weight in mixture ethanol/water (54.2/45.8% weight) at cooling rates of 1 and 14 °C h^{-1}.

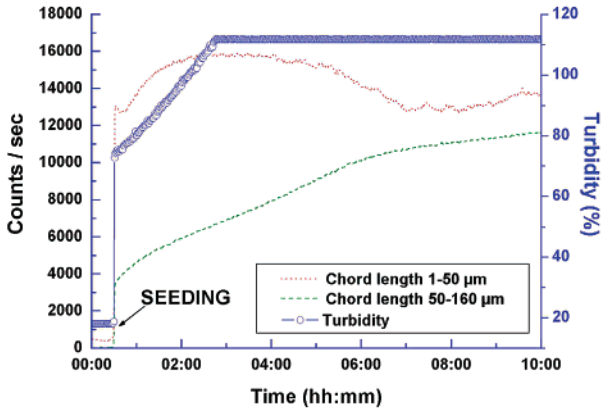

Figure 8. Turbidity and chord length distribution versus time of a seeded drug solution concentrated to 14.6% weight in mixture ethanol/water (54.2/45.8% weight) at 40 °C (point A in Figure 2).

light scattering at 90° in quiescent medium[11] (Figure 2). There is no difference between the data, indicating as expected that in both cases, stirred and quiescent media, we measured the equilibrium liquid−liquid coexistence curve. The advantage of FBRM on turbidity measurements is the possibility to measure different chord length (CL) versus temperature. We show, in Figure 5, that when the temperature is decreased below the cloud point the number of counts for the CL 1−20 μm increases, corresponding to the droplet nucleation. After this nucleation, the number of counts in CL fraction 20−50 and 50−100 μm increase, which characterizes the droplet growth and coalescence. This is confirmed by direct observation with the in-process PVM probe (Figure 6); because of the high-droplet concentration and the movement inside the crystallizer due to the stirring it is difficult to obtain quantitative information on the mechanism of droplet enlargement, namely, by growth or coalescence.

3.1.2. Influence of the Cooling Rate on the Cloud Point. In industrial crystallization, it is well-known that the larger the cooling rate the larger the metastable zone width for nucleation.[19] We show, in Figure 7, that it is also true for the demixion; when the cooling rate is increased from 1 to 14 °C h^{-1} the cloud point is decreased 1 °C.

To conclude this part, it is noteworthy that no primary nucleation was observed in the time frame of the experiments, whereas the solution was supersaturated with respect to both polymorphs FI and FII. As a result, LLPS prevents drug primary nucleation.

3.2 Characterization of the Impact of the LLPS on the Crystallization by Seeding. In most of the industrial process, the nucleation is controlled by seeding; here we study the impact of the LLPS on the crystallization by seeding in a 200-mL stirred batch-crystallizer.

These crystallization experiments are monitored by turbidity and FBRM probes. The seeding is performed with crystals of FI (size < 50 μm); this is the so-called "seeding the desired polymorph".[14] In all cases, crystals obtained at the end of the experiment are of FI.

3.2.1. Seeding between Solubility and Demixing Curves (Point A in Figure 2). A solution of $C_{35}H_{41}Cl_2N_3O_2$ at a concentration of 14.6% weight at 60 °C was cooled to 40 °C (point A in Figure 2). This point is in the metastable zone for nucleation, the seeding is performed at 40 °C, and the temperature is kept constant throughout the experiment. Results are presented in Figure 8. At the seeding point the solution is clear, and after the seeding the turbidity of the suspension increases instantaneously from 10 to 78% and increases continuously for the next 2 h, 30 min until saturation of the signal. This continuous increment expresses the secondary nucleation and the growth of crystals. The FBRM probe gives more information; for 30 min, after the seeding, a small decrease and a plateau are observed for the CL 1−50 μm, whereas the CL 50−160 μm increases. The seed is growing, but no nucleation is observable. At 30 min after the seeding the CL 1−50 μm increases due to the secondary nucleation. Finally, after 2 h, 30 min the CL 1−50 μm decreases slowly due to the end of the nucleation.

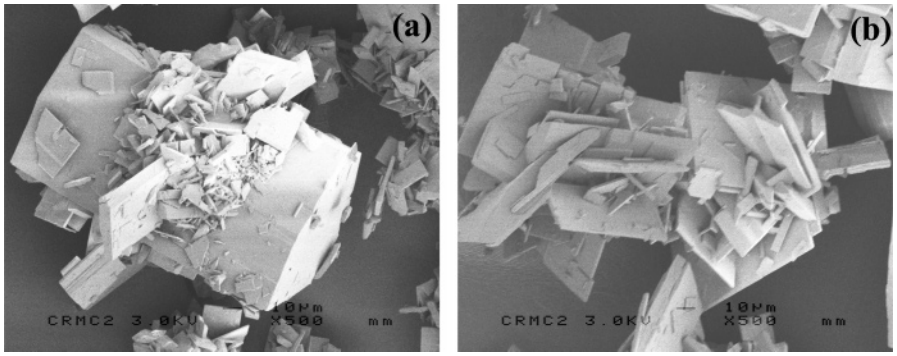

Figure 9. SEM photographs of crystals obtained in experiment (a) outside the demixion zone and (b) inside the demixion zone.

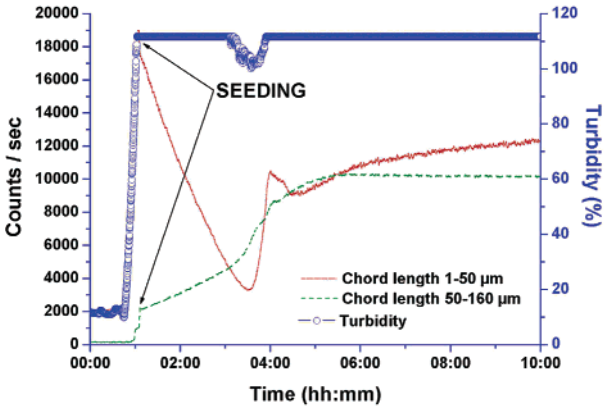

Figure 10. Turbidity and chord length distribution versus time of a seeded drug solution concentrated to 14.6% weight in mixture ethanol/water (54.2/45.8% weight) at 30 °C (point B in Figure 2).

During all the experiments the CL 50−160 μm increases due to the crystal growth. Typical crystals obtained from this experiment are presented in Figure 9a; here we observe an important heterogeneous nucleation on the seed. We can propose the following mechanism for the secondary nucleation, contact nucleation by surface breeding:[20] (1) heterogeneous nucleation and growth on the parent crystals and (2) formation of secondary fragment due to collisions between two crystals or between a crystal and a part of the apparatus. During the first 30 min of the experiment, where no nucleation was detectable by FBRM, only a few nuclei were removed from the parent crystal. To conclude, in the case of seeding in the metastable zone for nucleation and outside the demixion zone, we observe the classical growth and secondary nucleation mechanisms.

3.2.2. Seeding in the Demixion Zone (Point B in Figure 2). A solution of $C_{35}H_{41}Cl_2N_3O_2$ at a concentration of 14.6% weight at 60 °C was cooled to 30 °C (point B in Figure 2). This point is in the LLPS or demixion zone between the binodal and the spinodal curves; the seeding is performed at 30 °C, and the temperature is kept constant throughout the experiment. Results are presented in Figure 10. As a result of the LLPS, the turbidity signal is saturated before the seeding.

In the first stage (from $t = 0$ to 2 h, 30 min, $t = 0$ is the seeding time), looking at the FBRM data, the CL 1−50 μm starts to decrease just after the seeding and the CL 50−160 μm increases due to the growth of crystals and/or droplets. The CL 1−50 μm reaches a minimum at $t = 2$ h, 30 min. Interestingly, we note the cross-correlation between the turbidity and the FBRM data at $t = 2$ h, 30 min; a decrease of the suspension turbidity is observed due to the diminution of the number of crystals and/or droplets of size below 50 μm.

In the second stage (from $t = 2$ h, 30 min to 3 h, 30 min), the CL 1−50 μm starts to increase corresponding to a nucleation of crystals and/or droplets.

In the third and last stage ($t > 3$ h, 30 min), crystals and droplets grow, and the solute concentration decreases and reaches the liquid−liquid coexistence curve so that crystals grow at the expense of the droplets and the droplets disappear, and secondary nucleation starts. This means a waiting period for secondary nucleation due to the LLPS. Typical crystals obtained from this experiment are presented in Figure 9b; the crystal habit is the same, but the size is different.

Turbidity and FBRM monitoring do not allow separation of crystal and droplet evolution in the suspension.

With a view to interpreting the different phenomena that occur in suspension, we observe a solution seeded, in a 2-mL quiescent thermostated crystallizer, under a video microscope. Because the suspension is not stirred and to avoid a fast macroscopic gravity-driven separation into two phases, the experiment is carried out at 35 °C (point C in Figure 2, note that this point is in the same part of the phase diagram as the point B: in the demixion zone between the binodal and the spinodal curves, LLPS proceeds by a nucleation and growth mechanism[21] in both experiments). In Figure 11a, we observe droplets and a crystal at the beginning of the experiment. After 6 h, we characterize the growth of the crystal as well as the growth and the coalescence of the droplets. The new crystal in Figure 11b is not due to nucleation; this crystal was introduced in the volume of the crystallizer by the seeding and because of its size it took a longer time before it reached the bottom of the crystallizer. The coalescence of droplets is confirmed by their decreasing number (compare Figure 11, panels a to b and c). Crystals were still growing and we observed a nucleation of droplets by an heterogeneous mechanism (Figure 11c−f).

To conclude, in the case of seeding in the demixion zone, the first stage is the growth of crystals as well as the growth and coalescence of droplets. In the second stage, crystals and droplets are still growing and droplet heterogeneous nucleation occurs. In the last stage, droplets disappear and the secondary nucleation starts. Despite the large supersaturation, the nucleation is hindered until the solution concentration reaches the liquid−liquid coexistence curve.

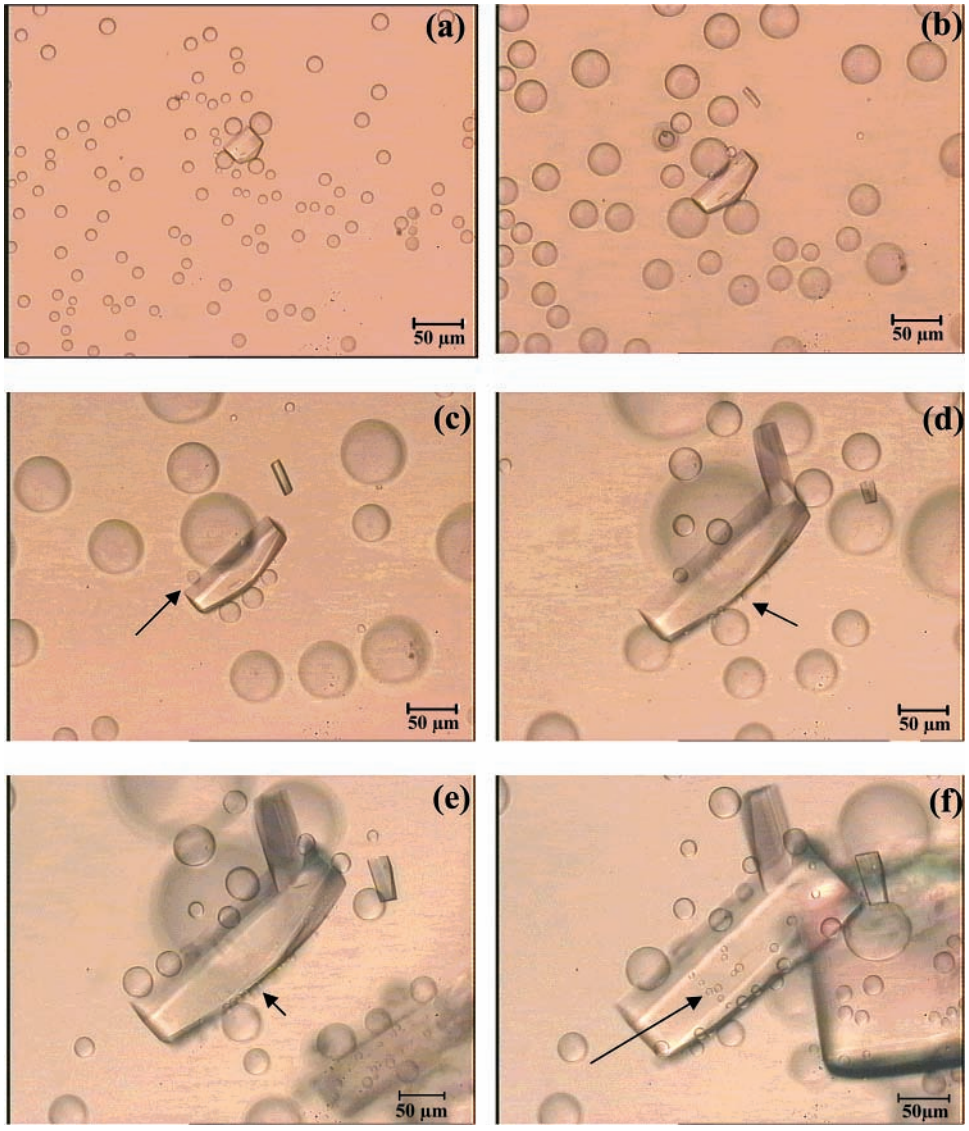

Figure 11. In situ observations under optical microscopy of seeding with polymorph FI of drug solution concentrated to 14.6% weight in mixture ethanol/water (54.2/45.8% weight) at 35 °C (point C in Figure 2), (a) $t = 0$, (b) $t = 6$ h, (c) $t = 12$ h, (d) $t = 22$ h, (e) $t = 30$ h, and (f) $t = 32$ h. (The arrow indicates the heterogeneous nucleation of droplets onto the crystal surface.)

4. Conclusion

In this paper, we monitor drug crystallization experiments by seeding by in situ turbidity and FBRM. By coupling video microscopy to these experiments, we visualize crystal and droplet evolution. Practically, the turbidity probe is good tool to detect an event such as a nucleation, a dissolution, or an aggregation;[22,23] here we detect droplet nucleation. However, FBRM is a more complete probe because it measures particle size in situ and in real time.

In the case of seeding experiments in the metastable zone for nucleation and outside the demixion or LLPS zone, we observe the classical growth and secondary nucleation mechanisms.

In the case of seeding experiments in the LLPS zone, the first stage is the growth of crystals as well as the growth and coalescence of droplets. In the second stage crystals and droplets are still growing and droplet heterogeneous nucleation occurs. In the last stage, droplets disappear and the secondary nucleation starts.

Finally, LLPS changes the medium and the conditions of crystallization, prevents the drug nucleation, both primary and secondary, and consequently affects the process. Depending on the point of seeding in the phase diagram, inside or outside the liquid−liquid-phase separation region, the crystallization mechanisms and kinetics are different.

Acknowledgment. The authors are indebted to SANOFI-SYNTHELABO for financial support, and to T. Bactivelane and M. C. Toselli for technical assistance.

References

(1) Anderson, V. J.; Lekkerkerker, H. N. W. *Nature* **2002**, *416*, 811.
(2) Asherie, N.; Lomakin, A.; Benedek, G. B. *Phys. Rev. Lett.* **1996**, *77*, 4832.
(3) Wolde, P. R.; Frenkel, D. *Science* **1997**, *277*, 1975.
(4) Noro, M. G., K. N.; Frenkel, D. *Europhys. Lett.* **1999**, *48*, 332.
(5) Veesler, S.; Lafferrere, L.; Garcia, E.; Hoff, C. *Org. Proc. Res. Dev.* **2003**, *7*, 983.

(6) Maeda, K.; Aoyama, Y.; Fukui, K.; Hirota, S. *J. Colloid Interface Sci.* **2001**, *234*, 217.
(7) Broide, M. L.; Tominc, T. M.; Saxowsky, M. D. *Phys. Rev. E* **1996**, *53*, 6325.
(8) Grouazel, S.; Perez, J.; Astier, J.-P.; Bonneté, F.; Veesler, S. *Acta Crystallogr.* **2002**, *D58*, 1560.
(9) Lafferrere, L.; Hoff, C.; Veesler, S. *Eng. Life Sci.* **2003**, *3*, 127.
(10) Bonnett, P. E.; Carpenter, K. J.; Dawson, S.; Davey, R. J. *Chem. Commun.* **2003**, 698.
(11) Lafferrere, L.; Hoff, C.; Veesler, S. *J. Cryst. Growth* **2004**, *269*, 550.
(12) Galkin, O., Vekilov, P. G. *Proc. Natl. Acad. Sci. U.S.A.* **2000**, *97*, 6277.
(13) Vivares, D.; Bonnete, F. *J. Phys. Chem. B* **2004**, *108*, 6498.
(14) Beckmann, W. *Org. Proc. Res. Dev.* **2000**, *4*, 372.
(15) Monnier, O.; Klein, J. P.; Hoff, C.; Ratsimba, B. *Part. Part. Syst. Charact.* **1996**, *13*, 10.
(16) Braatz, R. D. *Annu. Rev. Control* **2002**, *26*, 87.
(17) Fujiwara, M.; Chow, P. S.; Ma, D. L.; Braatz, R. D. *Cryst. Growth Des.* **2002**, *2*, 363.
(18) Dowding, P. J.; Goodwin, J. W.; Vincent, B. *Colloids Surf., A* **2001**, *192*, 5.
(19) Lewiner, F.; Klein, J. P.; Puel, F.; Févotte, G. *Chem. Eng. Sci.* **2001**, *56*, 2069.
(20) Van Der Heijden, A. E. D. M.; Van Rosmalen, G. M. Industrial mass crystallisation. In *Handbook of Crystal Growth*; Hurle, D. T. J., Ed.; North-Holland: Amsterdam, 1994; Vol. 2; p 315.
(21) Lupis, C. H. P. *Chemical Thermodynamics of Materials*; Elsevier Science: New York, 1983.
(22) Masy, J. C.; Cournil, M. *Chem. Eng. Sci.* **1991**, *46*, 693.
(23) Groen, H.; Roberts, K. J. *J. Phys. Chem. B* **2001**, *105*, 10723.

CG0497750